Armenian Journal of Physics, 2016, vol. 9, issue 1, pp. 20-28

Characteristics of Electrodeposited ZnO Nanostructures: Size and Shape Dependence

Fatemeh Ebrahimi Tazangi[1], Ali Rahmati[1,2]

[1]*Departement of Physics, Faculty of Science , Vali-e-Asr University of Rafsanjan, Rafsanjan, Iran*
[2]*Nano-structures laboratory, Faculty of Science , Vali-e-Asr University of Rafsanjan, Rafsanjan, Iran*

E-mail: alirahmati1980@gmail.com

Received 25 February 2016

Abstract. Zinc oxide nanostructures were grown on Si (111) using a simple electrodeposition route. Crystalline structure, optical and morphological properties were studied using X-ray diffraction, reflectance and photoluminescence (PL) spectroscopy, and scanning electron microscopy (SEM), respectively. This work provides insight into the significance of deposition time on controlling the shape and size of ZnO structure and white emission. The thermally treated ZnO nanostructures show hexagonal wurtzite nanocrystalline structure (~10 nm). The quantum confinement effect and band filling have been discussed on optical band gap widening from 3.21 eV to 3.70 eV. The PL spectra have illustrated fundamental band-edge emission in UV region and defect emission in visible region.

Keywords: two electrode electrodeposition, quantum confinement effect, band filling

1. Introduction

Zinc oxide (ZnO) is a II–VI group semiconductor material with a hexagonal wurtzite crystal structure. ZnO is a n-type semiconductor with wide and direct bandgap of 3.37 eV (at 300 K), a large free-exciton binding energy (60 meV), a strong cohesive energy of 1.89 eV, a high optical gain (300 cm^{-1}), and high mechanical and thermal stabilities and radiation hardness. Thin films of zinc oxide are the object of quickly growing in the last few years because of transparency in the visible wavelength, high electrochemical stability, absence of toxicity, low cost, easy of mass production, stability at operating temperatures and good resistance to thermal shocks, oxidation, UV radiation. Due to these unique characteristics, it is expected ZnO's efficient utilization in different commercial applications such as integrated optics, antireflection coatings, liquid crystal displays, light emitting diodes, laser diodes, UV range detecting devices, chemical sensors, solar cells, photo degradation and photocatalysis, superhydrophobic and self-cleaning surfaces. ZnO is also a strong candidate for high temperature electronic devices that can reliably be operated in space and other harsh environments [1-3].

ZnO thin films have been synthesized by a variety of processes such as vapor–liquid–solid (VLS), chemical vapor deposition (CVD), electron beam evaporation, spray pyrolysis, hydrothermal and electrochemical deposition method [1-9]. The electrodeposition is a simple method, which presents several advantages such as: (1) easy control of the thickness and the morphology of the film, (2) simplicity, (3) low equipment cost, and (4) the possibility of making large area thin films, as well as to produce a variety of different morphological deposits [10]. The deposition process can be carried out on various substrates, such as glass, copper, ITO, polymers, semiconductors and templates. In this method two main electrolyte solutions are utilized: $Zn(NO_3)_2$ and $ZnCl_2$. The electrodeposition of ZnO is based on the generation of OH^- ions at the surface of working electrode by electrochemical cathodic reduction of precursors such as O_2, NO_3^- and H_2O_2 in zinc ions aqueous solution.

In the present experiments, ZnO films were cathodically deposited from zinc nitrate solutions. The zinc nitrate solution can act as both the zinc and oxygen precursor. The general scheme of eletrodeposition of ZnO from aqueous zinc nitrate solution is supposed as follows (Eqs. (1– 4)):

$$Zn(NO_3)_2 \rightarrow Zn^{2+} + 2NO_3^- \qquad (1)$$

$$NO_3^- + H_2O + 2e^- \rightarrow NO_2^- + 2OH^- \qquad (2)$$

$$Zn^{2+} + 2OH^- \rightarrow Zn(OH)_2 \qquad (3)$$

$$Zn(OH)_2 \rightarrow ZnO + H_2O \qquad (4)$$

Cathodic electrochemical reduction of nitrate to nitrite is catalyzed by Zn^{2+} ions that are adsorbed on the surface of the cathode and liberates hydroxide ions, as in Eqs. (1). Then, zinc ions precipitate with the hydroxyl anions, resulting in the formation of zinc hydroxide [4, 11]. During the electrodeposition, atmospheric air (as oxygen source) dissolved in the solution. The dissolved oxygen is essential for the oxide growth (ZnO) without oxygen deficient, once the negative potential is applied to the working electrode, the reaction will start. The deposition reaction in the electrolyte is as:

$$Zn^{+2} + \frac{1}{2}O_2 + 2e^- \rightarrow ZnO \qquad (5)$$

2.Experiment

2.1 Synthesis

ZnO coating were prepared by the electrochemical deposition (ECD) method from a electrolyte consisting of 0.17 M $Zn(NO_3)_2$ and for supporting electrolyte 0.01M KNO_3 (Merk, 99%) was employed to ensure a good conductivity in the aqueous solution. Aqueous solution maintained at constant temperature and voltage of 75^0C, 1.5V, respectively. Silicon substrates was used as working electrode (WE) and a platinum (Pt) was used as the counter electrode (CE) in a traditional two electrode cell for electrochemical deposition. Before deposition, the substrates were cleaned in acetone; ethanol then in deionized (DI) water for 10 min each in the ultrasonic bath and dried in an air flux. Afterwards, the substrates were immersed in electrolyte with different intervals of times: 2 h and 1h. The electrolyte was continuously stirring and air bubbling to provide oxygen presence in electrolyte medium. The produced samples were carefully rinsed with deionized water to remove nitrate salts and then were dried in a hot plate at 100^0C for 120 minutes. The prepared coatings were annealed at a temperature of 400^0C for 4 h in the ambient atmospheric condition using a controllable tube furnace.

2.2 Characterization

The surface morphology and the structure of the ZnO structures were investigated using scanning electron microscopy (EM3200 KYKY, SEM) and X-ray diffraction (Siemens D5000 XRD) using X- ray source with a wavelength of 0.1518 nm. Optical properties were investigated using Avantes spectrometer (Ava spec-2048 TEC).

3. Result and discussion

3.1 Structural properties

Fig 1 shows X-ray diffraction profile of electrodeposited ZnO coatings. The diffraction pattern of (002), (110) and (103) planes are observed. The diffraction peak intensity from (002) plane were increased from sample deposited for 1h to 2h. However, inverse trend was observed for (103) peak intensity. Lupan et al [1] and Jeong et al [12] showed that (100) peak in diffraction pattern of ZnO structure could be diminished.

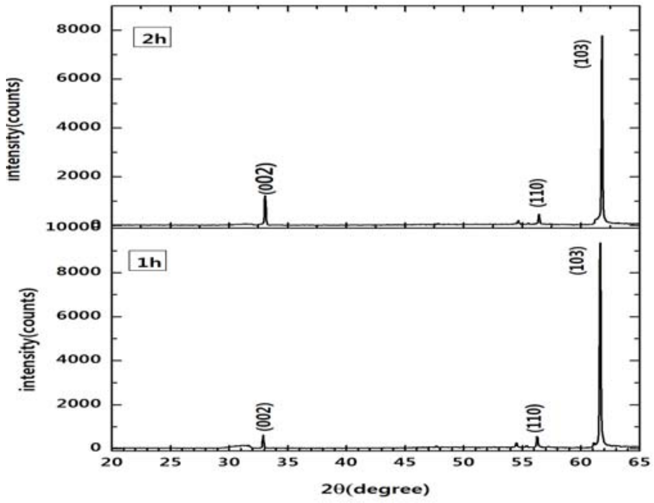

Fig. 1. XRD pattern of annealed ZnO coating deposited on (100) for 1 h and 2 h

The structure of annealed ZnO is hexagonal wurtzite with random orientation. The lattice constants were extracted from peak position using Bragg's law. Mean crystallite size (D) was calculated from strongest peak using Debye-Scherrer formula:

$$D = \frac{k\,\lambda}{\beta \cos\theta_{hkl}} \tag{6}$$

where λ=1.5418 Ǻ and β is full width at half maximum. The lattice constants and mean crystallite size are given in Table 1. The in-plane (a) and out-plane (c) lattice constants showed higher values than that of bulk ZnO (a=3.25 Ǻ and c=5.21 Ǻ) and ZnO thin films [1].

Table 1. Peak position, peak broadening, lattice constant and mean crystallite size of ZnO structure

Sample	2θ	hkl	FWHM (degree)	d (Ǻ)	a (Ǻ)	c (Ǻ)	D (nm)
1 h	32.91	(002)	0.1181	2.8393	3.36	5.27	12
	54.51	(110)	0.1181	1.6834			
	61.63	(103)	0.1181	1.5049			
2 h	33.09	(002)	0.1574	2.7075	3.26	5.31	11
	56.43	(110)	0.1181	1.6307			
	61.79	(103)	0.1181	1.5015			

The formation of SiO_x nanosheet on Si substrate induces lattice expansion in ZnO nanostructures. The mean crystallite size of ZnO structure is around 10nm.

3.2. Surface morphology

SEM images of ZnO structure are shown in Fig. 2. The sample grown at deposition time of 1h has spherical shape with well-known boundary. Its grain size is around 35nm. However, samples grown at deposition time of 2 and 3h are rod-like structure with nano- and micron size, respectively. As deposition time increase, the spherical ZnO structure elongate in an arbitrary direction to grow rod-like structure.

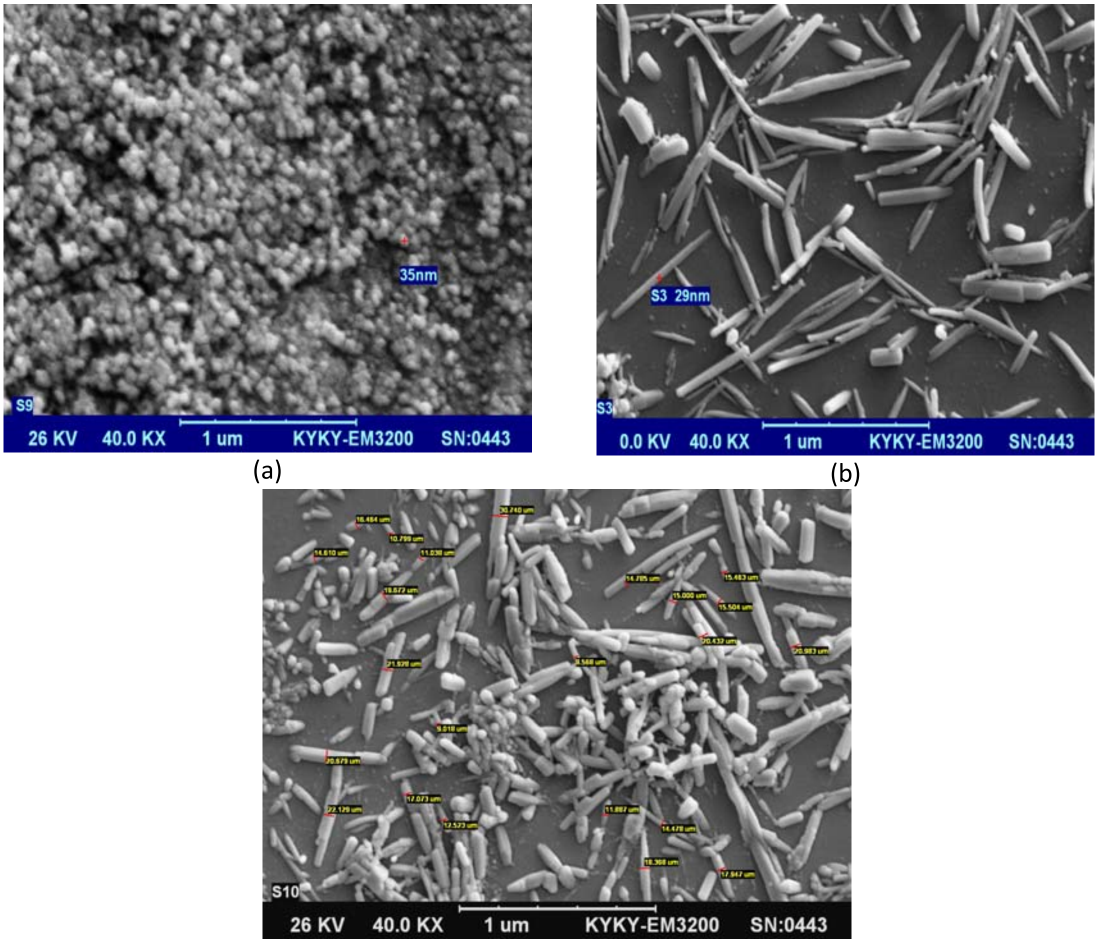

(a) (b)

(c)

Fig. 2. SEM images of annealed ZnO coating deposited on (100) for 1 h (a), 2 h (b) and 3 h (c)

3. 3 Optical properties

Fig. 3 shows the reflectance spectra of ZnO coatings on Si substrate. The corresponding wavelength of absorption shoulder is depicted in Fig. 3. The optical bandgap energy (E_g) is calculated from

$$E_g = \frac{1240 eV.nm}{\lambda(nm)} \tag{7}$$

The sample grown for 1h has bandgap of 3.34 eV, but the bandgap energy is 3.70 eV for the sample grown for 2 h. It is worthily noticed the diameter of spherical and rod-like grains are around 35 nm and 29 nm for the deposition time of 1 h and 2 h, respectively. This is due to stretching of ZnO in one-dimension as deposition time increases from 1 h to 2 h. As deposition time increases, the bandgap of ZnO was decreased due to removal of quantum confinement effects. The bandgap energy is around that of bulk ZnO for the sample grown for 3 h.

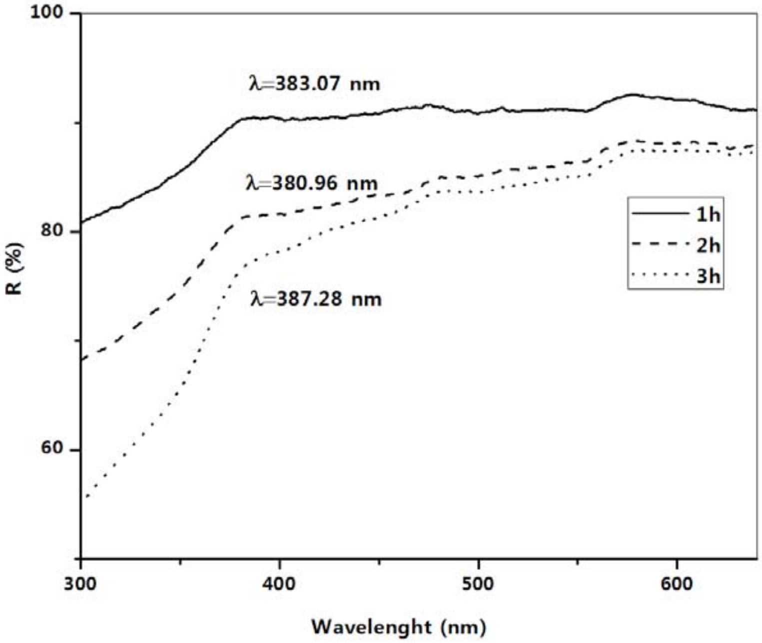

Fig. 3. Reflectance spectra of annealed ZnO coating deposited on (100) for 1 h, 2 h and 3 h

3.4 Photoluminescence

Photoluminescence (PL) is a technique, which can provide data related to defect levels, and the ratio IUV/IDL (the intensity of the ultraviolet to the visible deep level related luminescence) is a measure of defect states in ZnO material. Figure 4 shows the room temperature PL spectra for the studied samples annealed at temperature of 400^0C. On the PL spectra, an ultraviolet (UV) emission and a broad visible emission band are observed for the as grown ECD ZnO film. The UV emission line for the as-grown ZnO films peaking at 380 nm is attributed to a free-exciton and a neutral donor bound exciton. As deposition time increases, the UV exciton-related emission peak is weakly red-shifted. These results essentially agree with the analysis results of the shift of the optical absorption edge. Thus, the red shift of the optical bandgap and the improved UV emission after long deposition time can be due to the improved crystallinity of the ECD ZnO film and reduced defects (donor) concentration in the film. It can also be due to NO_2^- content reduction in ZnO films after the thermal treatment.

The FWHM values of the UV peaks are around 15 to 20 nm. Defect concentrations decrease with deposition time of ECD ZnO. Therefore, the intensity of visible PL emission increases and UV emission decreases, correspondingly. For long deposition time, the visible peak is hardly observed from the insert in Fig. 4.

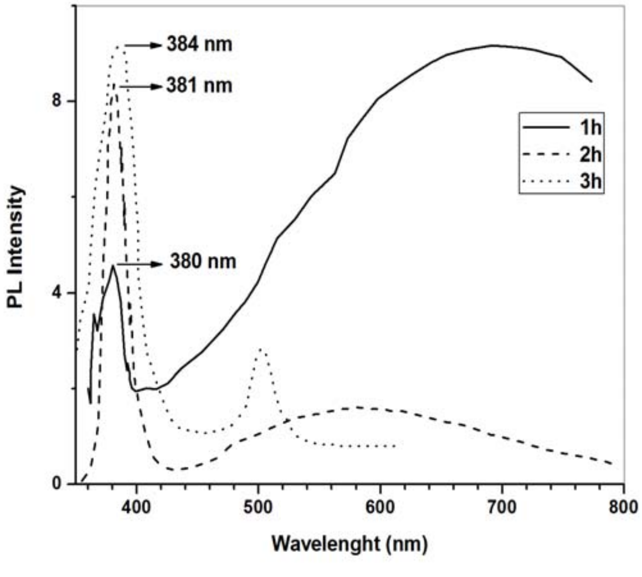

Fig. 4. Photoluminescence spectra of annealed ZnO coating deposited on (100) for 1 h, 2 h and 3 h

The intensity ratio between the near-band-edge UV emission and the visible is usually used to evaluate the quality of ZnO. This ratio was found to be equal to 0.4, 4 and 5 for the deposition time of 1 h, 2 h and 3 h, respectively.

Conclusion

ZnO coatings were deposited on Si (111) using electrodeposition technique. Crystalline structure, morphological, optical and photoluminescence properties of the annealed structure of ZnO were studied. The nano-crystalline coatings have a hexagonal wurtzite structure with random orientation. The deposition time affect on shape and size of the grown structure, in particularly, as deposition time increases, the shape of ZnO structure changes from sphere-like structure to rod-like ones. Quantum size effect causes to widening of bandgap energy from 3.21 to 3.7 eV. The PL spectra have two parts; fundamental band-edge emission in UV region and defect emission in visible region.

References

[1**].** Lupan O., Pauporte T., Chowv, Viana B., Pelle F., Ono L. K., Roldan Cuenya B., Heinrich H. Effects of annealing on properties of ZnO thin films prepared by electrochemical deposition in chloride medium. *Applied Surface Science*. 2010, 256, 1895–1907

[2] Lupan O., Guerin V.M., Tiginyanu I.M., Ursaki V.V., Chow L., Heinrich H., Pauporte T. Well-aligned arrays of vertically oriented ZnO nanowires electrodeposited on ITO-coated glass and their integration in dye sensitized solar cells. *Journal of Photochemistry and Photobiology A: Chemistry*. 2010, 211, 65–73

[3] Li G. R., Dawa C. R., Lu X. H., Yu X. L., and Tong Y. X. Use of Additives in the Electrodeposition of Nanostructured Eu^{3+}/ZnO Films for Photoluminescent Devices. *Langmuir.* 2009, *25,* 2378-2384

[4] Chen Z., Tang Y., Zhang L., Luo L. Electrodeposited nanoporous ZnO films exhibiting enhanced performance in dye-sensitized solar cells. *Electrochimica Acta*. 2006, 51, 5870–5875

[5] Garces N. Y., Wang L., Bai L., Giles N. C., and Halliburton L. E. Role of copper in the green luminescence from ZnO crystals. *Appl. Phy. Lett.* 81 (4), 2002, 622- 624

[6] Han Z., Li S., Chu J., and Chen Y. Controlled growth of well-aligned ZnO nanowire arrays using the improved hydrothermal method. *Journal of Semiconductors*. 2013, 34(6), 063002-1- 063002-6

[7] Salaken S. M., Farzana E., and Podder J. Effect of Fe-doping on the structural and optical properties of ZnO thin films prepared by spray pyrolysis. *Journal of Semiconductors*. 2013, 34 (7), 073003-1- 073003-6

[8]. Muthukumar P., Selvakumari T. M., Ganesan S. Structural and optical properties of nanostructures zinc oxide thin films. *Digest Journal of Nanomaterials and Biostructures.* 2010, 5(3), 635-639

[9]. Wang Q. G, Wang G. Z., Jie J. S., Han X. H., Xu B., Hou J.G. Annealing effect on optical properties of ZnO films fabricated by cathodic electrodeposition. *Thin Solid Films*. 2005, 492, 61 – 65

[10]. Kathalingam A., Kim M. R., Chaeand Y. S., Rhee J. K. Studies on electrochemically deposited ZnO thin films. *Journal of the Korean Physical Society*. 2009, 55 (6), 2476- 2481

[11] Li L., Pan S., Dou X., Zhu Y., Huang X., Yang Y., Li G., and Zhang L. Direct Electrodeposition of ZnO Nanotube Arrays in Anodic Alumina Membranes. *J. Phys. Chem. C.* 2007, *111*, 7288-7291

[12] Jeong S. S., Mittiga A., Salza E., Masci A., Passerini S. Electrodeposited ZnO/Cu2O heterojunction solar cells. *Electrochimica Acta*. 2008, 53, 2226–2231.